Letter

Fractional quantum Hall states with variational projected entangled-pair states: A study of the bosonic Harper-Hofstadter model

Erik Lennart Weerda [*]
Institute for Theoretical Physics, University of Cologne, D-50937 Köln, Germany

Matteo Rizzi
Institute for Theoretical Physics, University of Cologne, D-50937 Köln, Germany
and Forschungszentrum Jülich GmbH, Institute of Quantum Control, Peter Grünberg Institut (PGI-8), 52425 Jülich, Germany

(Received 10 October 2023; accepted 28 May 2024; published 26 June 2024)

An important class of model Hamiltonians for investigation of topological phases of matter consists of mobile, interacting particles on a lattice subject to a semiclassical gauge field, as exemplified by the bosonic Harper-Hofstadter model. A unique method for investigations of two-dimensional quantum systems are the infinite projected-entangled pair states, as they avoid spurious finite-size effects that can alter the phase structure. However, due to no-go theorems in related cases, this was often conjectured to be impossible in the past. In this Letter, we show that upon variational optimization, the infinite projected-entangled pair states can be used to this end by identifying fractional Hall states in the bosonic Harper-Hofstadter model. The obtained states are characterized by showing exponential decay of bulk correlations, as dictated by a bulk gap, as well as chiral edge modes via the entanglement spectrum.

DOI: 10.1103/PhysRevB.109.L241117

Introduction. The physics of interacting topological phases of matter, which includes phenomenalike fractionally charged quasiparticles, exotic exchange statistics, and long-range (topological) entanglement has led to the formulation of many new concepts in physics, most notably topological order [1]. Additionally, using these phenomena offers a promising route for robust quantum information technology [2,3]. The paradigmatic family of quantum states for these phases of matter are the fractional quantum Hall states [4,5] and their lattice generalization as fractional Chern insulators [6]. Given this, an enormous amount of theoretical effort, driven by the fundamental interest in the fractional quantum Hall states, has been put forward since their discovery and continues to this day. Moreover, with recent advances, in capabilities of experiments on cold atoms like the possibility to include artificial gauge fields, have put the extremely rich physics of fractional Hall states into the grasp of current technologies [7–11]. Recently, a crucial first experimental step was made with the realization of a Laughlin state of two atoms in such an experiment [12]. A major part of the quest for the realization of fractional quantum Hall physics in well-controlled synthetic quantum matter experiments is the identification of specific Hamiltonians where these phases arise. As these states generically emerge from an intricate interplay of magnetic fields and interactions between the particles, the candidate Hamiltonians are challenging for state-of-the-art numerical methods to treat. Within the class of tensor network methods for such numerical studies, the infinite projected entangled-pair state (iPEPS) [13] framework has unique advantages for this task. As it operates directly in the thermodynamic limit in two dimensions, it can eliminate finite-size effects that can significantly bias other related methods, e.g., cylinder-matrix-product states (MPS), leading to possibly altered phase boundaries or even artificial phases that are nonexistent in the two-dimensional limit. Thus, the iPEPS ansatz constitutes an important tool for the determination of the phase structure of many-body Hamiltonians. However, doubts have been raised about the general applicability of the PEPS ansatz for the numerical simulation of gapped chiral states because of a no-go theorem for the case for free fermions [14]. In a recent work, this issue was studied more closely from a numerical perspective [15]. It was shown that for a truncated parent Hamiltonian of a chiral spin liquid [16,17] the iPEPS ansatz was indeed successful in finding and representing this ground state numerically.

In this Letter, we take a further step in utility of the iPEPS framework by treating mobile bosons in an external gauge field, showing that chiral gapped topological phases arise. We are able to treat flux values that are in the range of today's experimental technology. With this, we demonstrate that this truly two-dimensional method can be applied beyond truncated parent Hamiltonians and can, in fact, tackle realistic models of experimental relevance. This setting necessitates the use of large unit cells in the iPEPS ansatz due to the magnetic unit cell over which the Hamiltonian terms vary due to the external gauge field. Crucial for this investigation is the fact that we make use of a fully variational ground-state search, as attempts with simple imaginary time

[*]Contact author: weerda@thp.uni-koeln.de

evolution turn out to yield inconclusive results. By scanning through different parameter values of the Harper-Hofstadter Hamiltonian, we are able to find incompressible plateaus at the filling fraction expected for bosonic fractional Hall states. We focus on the paradigmatic case of the Laughlin state in the case of hard-core bosons, but show that also for soft-core bosons and higher fillings we can find incompressible plateaus corresponding to more exotic fractional Hall states. The chiral nature of these states is verified with the use of the entanglement spectrum. We thus represent bosonic fractional quantum Hall states with PEPS.

Model and methods. We study a two-dimensional system of bosonic particles on a square lattice, which are interacting on site and are subject to a magnetic flux ϕ through each plaquette of the lattice. This situation is described by an interacting Harper-Hofstadter Hamiltonian

$$\hat{H} = -t\sum_{\langle ij\rangle}(e^{iA_{ij}}\hat{a}_i^{\dagger}\hat{a}_j + \text{H.c.}) - \mu\sum_i \hat{n}_i + \frac{U}{2}\sum_i \hat{n}_i(\hat{n}_i - 1), \tag{1}$$

in which the hopping amplitude t is dressed by the semiclassical gauge field. The gauge field is chosen such that it produces the desired magnetic flux per plaquette, $\phi = \sum_{\square} A_{ij}$. This Hamiltonian can be realized in cold atom experiments [8,9,11] and was the basis for the recent preparation of a two-body fractional quantum Hall state [12]. In the limit of large fillings, it also describes the physics of Josephson junction arrays [18].

For low densities and small values of ϕ, where the magnetic length $\ell_B = 1/\sqrt{\phi}$ is much larger than the lattice spacing, we approach the continuum setting, in which the presence of bosonic fractional Hall states is well established [19]. However, at large flux values at which current cold atom experiments can operate and lattice effects play a central role, the presence of truly lattice versions of the fractional quantum Hall states in the phase diagram remains a question of ongoing research. Studies based on exact diagonalization [20–28] as well as (infinite) density matrix renormalization group [(i)DMRG] [29–33] and tree-tensor networks (TTNs) [34,35] have suggested a multitude of fractional quantum Hall states in such systems. Even though these methods can provide insight into the possible phases of the Hamiltonian in the two-dimensional thermodynamic limit, it is widely acknowledged that they suffer from strong finite-size effects. In particular, for elongated cylinder geometries, as usually employed by the (i)DMRG methods of treating two-dimensional Hamiltonians, these strong finite-size effects lead to an overestimation of the stability of gapped phases as well as the emergence of charge density wave orders, breaking translation invariance, as discussed in Refs. [31,33]. Generically, it is not clear what the influence of finite-size effects is on all the possible low-energy phases close to the true ground state is. Thus, if these phases are in close competition, the phase with the energetically most favorable finite-size effect can be accidentally identified as the ground state. The circumstances where these considerations can become crucial include quite important models like the doped Hubbard model or models relevant for the search for spin liquids in materials, just to name a few.

Here, we thus aim to provide important clarification on the situation by showing that the iPEPS ansatz, using variational optimization, is capable of tackling such problems directly in the thermodynamic limit, and hence without spurious finite-size effects. The iPEPS ansatz [13,36] for the many-body wave function used in this investigation is parameterized by a set of tensors $(A_{1,1}, \ldots A_{m,n})$ that form a $m \times n$ unit cell (illustrated with the grey line) which is periodically repeated on the infinite lattice:

$$|\Psi(A_{1,1},\ldots,A_{m,n})\rangle = \sum_{\{n_i\}} C_{\{n_i\}}(A_{1,1},\ldots,A_{m,n})\,|\{n_i\}\rangle,$$

$C_{\{n_i\}}(A_{1,1},\ldots,A_{m,n}) =$

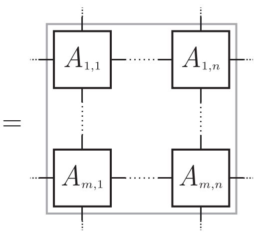

, (2)

The individual tensors $A_{i,j}$ are rank-5 tensors with four virtual indices of bulk (bond) dimension χ_B as well as a physical index whose dimension, d, is that of the local Hilbert space of the physical system. To contract this infinite tensor network for the calculation of norms and expectation values, we make use of the corner transfer matrix renormalization group (CTMRG) method [37–44]. The CTMRG is a power method that generates effective environments approximating the contraction of subsections of the infinite tensor network. The accuracy of this approximation is controlled by the bond dimension of the environment tensors, which we call the *environment bond dimension* χ_E. Beyond the calculation of expectation values, the environment tensors generated with the CTMRG method can also be utilized in other ways, e.g., in the evaluation of the entanglement spectrum [45,46], cf. Supplemental Material [47].

To allow us to treat more complicated Hamiltonians with a semiclassical gauge field and (large) magnetic unit cell and hosting chiral topological ground states with iPEPS, we need to perform a variational ground-state search. Within the ansatz class of iPEPS of a fixed unit cell size and bond dimension χ_B, the variational state optimization [48,49] using automatic differentiation [50], implemented as explained in Ref. [51], allows us to find the optimal approximation of the ground state. This variational framework for iPEPS has been advantageous in treating e.g., frustrated spin systems, including, recently, spin liquids [15,52–54]. For Hamiltonians, as in Eq. (1), a treatment using the alternative methods based on imaginary-time evolution (simple update) did not yield useful results. This further illustrates the importance of the framework of variational optimization of the iPEPS ansatz.

Results. We initially consider the $U \to \infty$ limit of hardcore bosons with a flux of $\phi = \pi/2$ per plaquette. Note, that for this choice of flux, the noninteracting Hamiltonian has remarkably flat lowest and highest bands, making it a promising choice for exhibiting fractional quantum Hall physics. The flatness of a band can be quantified by the ratio of its gap to the next band and its bandwidth [55–57]. Further, this large choice of flux is within reach of current cold-atom experiments [7–12,58]. To search for fractional Hall states in this model, we first map out the average occupation per site $\langle\hat{n}\rangle$ of the ground state as a function of the chemical potential μ;

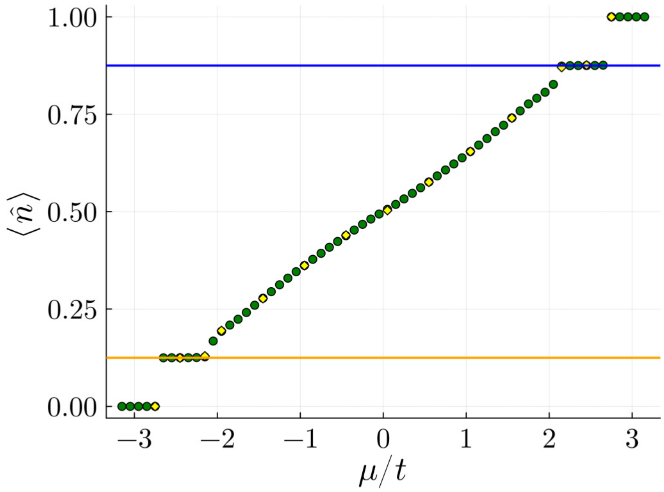

FIG. 1. Average occupation per site $\langle\hat{n}\rangle$ as a function of μ/t for hard-core bosons with bond dimensions $\chi_B = 4$ (green circles) and $\chi_B = 5$ (yellow diamonds). Note that the two incompressible plateaus are found at the filling expected for the $\nu = 1/2$ Laughlin state and its hole analog. The regime given by the fractional Hall plateaus makes up more than 20% of the parameter space in between the empty and completely filled state.

see Fig. 1. The calculations were performed with bulk bond dimensions $\chi_B = 4$ and $\chi_B = 5$ and values of environment bond dimension up to $\chi_E = 120$, which showed converged behavior for the observables, as shown in Fig. 1. We used the Landau gauge for the vector potential in Eq. (1) and multiples of the 4×1 magnetic unit cell for the unit cell of the iPEPS ansatz, cf. Supplemental Material [47] for more details on gauge choices and unit cells used in this Letter [47]. We find two incompressible plateaus in the occupation, one at low and one at high filling. The states on these plateaus show a homogeneous density. The average occupation of the lower plateau corresponds exactly to the occupation for a $\frac{2\pi\langle\hat{n}\rangle}{\phi} = \nu = 1/2$ Laughlin state of bosons. We observe a symmetry of occupation around $\mu = 0$, cf. Fig. 1. This can be understood by relating the Hamiltonian from Eq. (1) for a particular choice of flux and chemical potential $\hat{H}(\phi, \mu)$ to the same Hamiltonian with reversed sign for the chemical potential $\hat{H}(\phi, -\mu)$ using a particle-hole transformation

$$O_{\mathrm{ph}} = \prod_i (a_i^\dagger + a_i) \tag{3}$$

as well as time reversal Θ. Applying these transformations results in

$$\Theta O_{\mathrm{ph}} \hat{H}(\phi, \mu) O_{\mathrm{ph}} \Theta^{-1} = \hat{H}(\phi, -\mu) - \mu N, \tag{4}$$

with N the number of sites in the system. This also relates the eigenstates of $\hat{H}(\phi, \mu)$ and $\hat{H}(\phi, -\mu)$ and hence can be used to understand the precise nature of the plateau at the high filling of Fig. 1 as a Laughlin state of holes at hole-filling $\bar{\nu} = \frac{2\pi\langle\hat{n}_{\mathrm{h}}\rangle}{\phi} = 1/2$, with $\langle\hat{n}_{\mathrm{h}}\rangle = 1 - \langle\hat{n}\rangle$. We note further that the incompressible plateaus in Fig. 1 make up more than 20% of the parameter space between the empty and filled states. We attribute the fact that these plateaus make up such a sizable fraction to the flatness of the lower and upper bands of the Hamiltonian at $\phi = \pi/2$.

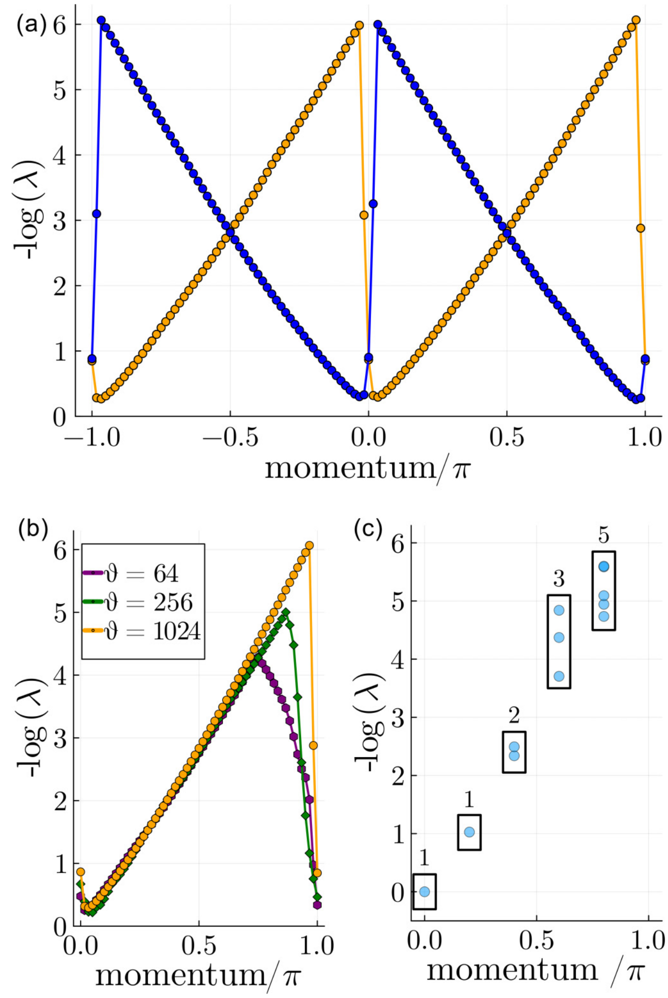

FIG. 2. (a) The orange dots show the low-lying part off the entanglement spectrum of a state on the incompressible plateau at low filling in Fig. 1. We clearly find a chiral entanglement spectrum indicating that this is a fractional quantum Hall state. The blue dots show the low-lying part off the entanglement spectrum of a state on the incompressible plateau at high filling with reversed chirality. (b) The low-lying part of the entanglement spectrum is shown for three values of the approximation parameter ϑ, illustrating that we can systematically increase the chirality of the entanglement spectrum. In our case, we have $\vartheta = \chi_E^2$. (c) Lowest branch of the entanglement spectrum on a ten-site cylinder. The counting associated with the chiral boson on the edge of the Laughlin state is observed.

We now characterize the properties of the states at the $\nu = 1/2$ filling to verify that this is indeed a chiral Laughlin state. We do so by first inspecting the entanglement spectrum, which should correspond to the gapless spectrum of the chiral edge modes, by following Li and Haldane [45]. The entanglement spectrum is defined as the spectrum of the entanglement Hamiltonian H_{ent} that, in turn, can be identified from the reduced density matrix ρ_l of a bipartition of the system $\rho_l = e^{-H_{\mathrm{ent}}}$. We can access the entanglement spectrum for our system by utilizing the bulk-boundary correspondence for PEPS [59] and do so directly in the thermodynamic limit [46] as well as on a cylinder of finite circumference. A more detailed description of the methods used for the computation

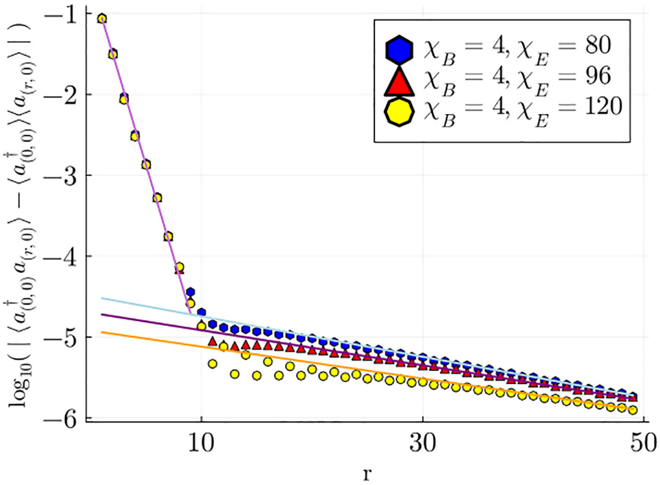

FIG. 3. Correlation function of the plateau state at low filling, cf. Fig. 1. At short distances, the correlations decay exponentially with distance, consistent with a bulk gap of the state. We extract a correlation length of $\xi/\ell_B = 1.19$ which is consistent with previous results [34]. At long distances, we find a small artificial tail of in the correlation functions that is due to the fact that we represent a chiral topological gapped state with PEPS.

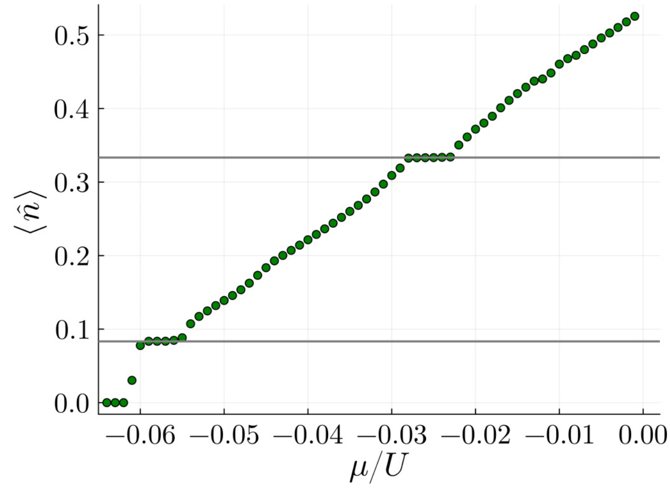

FIG. 4. Soft-core boson occupation per site for $\frac{U}{t} = 50$ and flux $\phi = \pi/3$. We see that an additional incompressible plateau at $\nu = 2$. The plateau at $\nu = 2$ corresponds to bosonic integer quantum Hall states.

and details on the approximations made can be found in the Supplemental Material [47].

In Fig. 2(a), we can see that we find an almost perfectly chiral entanglement spectrum for the states on the incompressible plateau at the $\nu = 1/2$ filling, confirming the chiral nature of the edge modes of the states on the incompressible plateaus in Fig. 1. The presence of the branch at negative momenta is due to the eigenvalues of the reduced density matrix with different particle numbers [60,61]. For the the states on the incompressible plateau at high filling, which we expect to be a Laughlin state of holes, we find that they have a chiral entanglement spectrum with reversed chirality, see Fig. 2(a), as expected for holes. The fact that the entanglement spectra shown here are not perfectly chiral at momentum zero stems from the numerical approximations made, but the chirality can systematically be improved by increasing the approximation parameter ϑ as illustrated in Fig. 2(b). This parameter corresponds to the bond dimension of the boundary Hamiltonian from the PEPS bulk-boundary correspondence, cf. Supplemental Material [47] for more information. We also perform the entanglement spectrum on a finite cylinder of circumference 10. This discretizes the edge spectrum and allows us to identify the degeneracy of the lowest energy edge excitations, cf. Fig. 2(c). These degeneracies (1, 1, 2, 3, 5,...) are the ones expected for chiral boson modes, the edge mode of the Laughlin state.

Additionally, we also calculate bulk correlation functions for the incompressible states at $\nu = 1/2$. As shown in Fig. 3, we find an exponential decay of correlations at short distances, consistent with the bulk gap of the Laughlin states, with a correlation length of $\xi/\ell_B = 1.19$ in units of the magnetic length $\ell_B = 1/\sqrt{\phi}$. This is compatible with the result obtained with tree tensor networks for finite systems at lower flux [34]. Furthermore, we observe a finite tail in the correlation function at long distances. This tail is a numerical artifact and can be identified as consequence of the fact that we are representing a gapped chiral state with PEPS: it has been observed as well in the context of related spin systems [15]. Increasing the environment bond dimension χ_E, for a fixed value of χ_B changes the details of the artificial long-range tail, while leaving the short-range exponentially decaying correlations invariant. We analyze the behavior of the long-range tails in more detail in the Supplemental Material [47].

To show that we are not limited to hard-core bosons, we relax the $U \to \infty$ condition and move to large but finite interactions $U/t = 50$. In our calculations, we allow up to two bosons per site in this case, given that even higher fillings are energetically strongly suppressed. In this situation, we observe, for a magnetic flux of $\phi = \pi/2$, a similar average occupation per site as in the case of hardcore bosons, with a slightly higher occupation at a given μ stemming from the fact that states including two bosons on a single site are now possible. We again find incompressible plateaus at $\nu = 1/2$ as well as at its hole analog, cf. Supplemental Material [47]. If we instead reduce the magnetic flux to $\phi = \pi/3$, we additionally find a plateau at filling factor $\nu = 2$, as shown in Fig. 4. This plateau is expected to be associated with exotic states that belong to the Jain sequence obtained in the composite fermion picture [62]. The $\nu = 2$ state from this sequence is a bosonic integer quantum Hall state, which is not intrinsically topological but rather a symmetry protected topological state [25,26,63–65].

Conclustion and outlook. In this Letter, we demonstrated that the variational iPEPS framework allows for the investigation of Hamiltonians of mobile, interacting particles with semiclassical gauge fields that host chiral topological states as ground states, such as fractional Hall states and Chern insulators. The iPEPS method is a crucial complement to other well-established methods for this task (such as exact diagonalization or other tensor network ansatzes) as it avoids finite-size effects that can alter the correct phase diagram.

Further, as it can give genuine information about the bulk physics, it can be used to benchmark whether finite-size experiments are actually displaying bulk behavior or are dominated by their boundary. The class of Hamiltonians describing mobile, interacting particles in a semiclassical gauge field, of which we have treated a paradigmatic example in this Letter, comes up in the description of several physical systems that have attracted enormous amounts of interest in recent years [8,12,66–69]. Furthermore, key characteristics, such as the importance of flat bands which aid the emergence of interesting correlated phases, are often shared among these different systems. In the bosonic Harper-Hofstadter model, the (relatively) flat bands of the Hamiltonian can be understood as leading to the prominence of interaction-driven physics and hence to fractional Hall states [6]. Correspondingly, in twisted bilayers systems the isolated moiré flat bands are the reason for many candidate ground states such as spin-liquid states, quantum anomalous Hall insulators, and chiral d-wave superconductors [70]. An important illustrative example is twisted WSe_2, which can be described by a moiré Hubbard model [71,72], in which the hopping on the triangular lattice is enhanced by a spin-dependent phase, tunable in experiments. Given the similarity of this Hamiltonian to the one studied in this Letter, this puts the investigation of the physics of twisted bilayer systems well within reach of the variational iPEPS framework, promising an unbiased numerical perspective on the physics of these systems. Furthermore, recent advances drastically improved the ability to calculate excitation spectra and structure factors in the variational iPEPS framework [73–75]. This allows direct connection to experimental results [76] and thus should clearly establish the variational iPEPS framework as a major tool of investigation in the above-mentioned systems.

Data corresponding to the numerical calculations in this work can be found in a Zenodo entry [77].

Acknowledgments. We thank P. Schmoll, N. Tausendpfund, M. J. Arildsen, and S. Trebst for discussions and the group of J. Eisert for warm hospitality during the visit supported by the CRC 183. E.L.W. thanks the Studienstiftung des deutschen Volkes for support. The authors warmly endorse the open source tensor network libraries of Quantum-Ghent group and acknowledge, in particular, the use of MPSKIT for the entanglement spectrum calculations. This work has been funded by the Deutsche Forschungsgemeinschaft (DFG, German Research Foundation) under Project No. 277101999—CRC 183 (Project No. B01). The authors gratefully acknowledge the Gauss Centre for Supercomputing e.V. [78] for funding this project by providing computing time through the John von Neumann Institute for Computing (NIC) on the GCS Supercomputer JUWELS at the Jülich Supercomputing Centre (JSC) (Grant NeTeNeSyQuMa) and the FZ Jülich for JURECA (institute Project No. PGI-8) [79].

[1] X.-G. Wen, *Colloquium*: Zoo of quantum-topological phases of matter, Rev. Mod. Phys. **89**, 041004 (2017).

[2] A. Y. Kitaev, Fault-tolerant quantum computation by anyons, Ann. Phys. **303**, 2 (2003).

[3] C. Nayak, S. H. Simon, A. Stern, M. Freedman, and S. Das Sarma, Non-Abelian anyons and topological quantum computation, Rev. Mod. Phys. **80**, 1083 (2008).

[4] D. C. Tsui, H. L. Stormer, and A. C. Gossard, Two-dimensional magnetotransport in the extreme quantum limit, Phys. Rev. Lett. **48**, 1559 (1982).

[5] R. B. Laughlin, Anomalous quantum Hall effect: An incompressible quantum fluid with fractionally charged excitations, Phys. Rev. Lett. **50**, 1395 (1983).

[6] S. A. Parameswaran, R. Roy, and S. L. Sondhi, Fractional quantum Hall physics in topological flat bands, C. R. Phys. **14**, 816 (2013).

[7] M. Aidelsburger, M. Atala, S. Nascimbène, S. Trotzky, Y.-A. Chen, and I. Bloch, Experimental realization of strong effective magnetic fields in an optical lattice, Phys. Rev. Lett. **107**, 255301 (2011).

[8] M. Aidelsburger, M. Atala, M. Lohse, J. T. Barreiro, B. Paredes, and I. Bloch, Realization of the Hofstadter Hamiltonian with ultracold atoms in optical lattices, Phys. Rev. Lett. **111**, 185301 (2013).

[9] H. Miyake, G. A. Siviloglou, C. J. Kennedy, W. C. Burton, and W. Ketterle, Realizing the Harper Hamiltonian with laser-assisted tunneling in optical lattices, Phys. Rev. Lett. **111**, 185302 (2013).

[10] M. Atala, M. Aidelsburger, M. Lohse, J. T. Barreiro, B. Paredes, and I. Bloch, Observation of chiral currents with ultracold atoms in bosonic ladders, Nat. Phys. **10**, 588 (2014).

[11] M. E. Tai, A. Lukin, M. Rispoli, R. Schittko, T. Menke, D. Borgnia, P. M. Preiss, F. Grusdt, A. M. Kaufman, and M. Greiner, Microscopy of the interacting Harper–Hofstadter model in the two-body limit, Nature (London) **546**, 519 (2017).

[12] J. Léonard, S. Kim, J. Kwan, P. Segura, F. Grusdt, C. Repellin, N. Goldman, and M. Greiner, Realization of a fractional quantum Hall state with ultracold atoms, Nature (London) **619**, 495 (2023).

[13] F. Verstraete and J. I. Cirac, Renormalization algorithms for quantum-many body systems in two and higher dimensions, arXiv:cond-mat/0407066.

[14] J. Dubail and N. Read, Tensor network trial states for chiral topological phases in two dimensions and a no-go theorem in any dimension, Phys. Rev. B **92**, 205307 (2015).

[15] J. Hasik, M. Van Damme, D. Poilblanc, and L. Vanderstraeten, Simulating chiral spin liquids with projected entangled-pair states, Phys. Rev. Lett. **129**, 177201 (2022).

[16] A. E. B. Nielsen, J. I. Cirac, and G. Sierra, Laughlin spin-liquid states on lattices obtained from conformal field theory, Phys. Rev. Lett. **108**, 257206 (2012).

[17] A. E. Nielsen, G. Sierra, and J. I. Cirac, Local models of fractional quantum Hall states in lattices and physical implementation, Nat. Commun. **4**, 2864 (2013).

[18] R. Fazio and H. Van Der Zant, Quantum phase transitions and vortex dynamics in superconducting networks, Phys. Rep. **355**, 235 (2001).

[19] N. Read and E. Rezayi, Beyond paired quantum Hall states: Parafermions and incompressible states in the first excited Landau level, Phys. Rev. B **59**, 8084 (1999).

[20] A. S. Sørensen, E. Demler, and M. D. Lukin, Fractional quantum Hall states of atoms in optical lattices, Phys. Rev. Lett. **94**, 086803 (2005).

[21] M. Hafezi, A. S. Sørensen, E. Demler, and M. D. Lukin, Fractional quantum Hall effect in optical lattices, Phys. Rev. A **76**, 023613 (2007).

[22] G. Möller and N. R. Cooper, Composite fermion theory for bosonic quantum Hall states on lattices, Phys. Rev. Lett. **103**, 105303 (2009).

[23] L. Mazza, M. Rizzi, M. Lewenstein, and J. I. Cirac, Emerging bosons with three-body interactions from spin-1 atoms in optical lattices, Phys. Rev. A **82**, 043629 (2010).

[24] A. Sterdyniak, N. Regnault, and G. Möller, Particle entanglement spectra for quantum Hall states on lattices, Phys. Rev. B **86**, 165314 (2012).

[25] Y.-C. He, S. Bhattacharjee, R. Moessner, and F. Pollmann, Bosonic integer quantum Hall effect in an interacting lattice model, Phys. Rev. Lett. **115**, 116803 (2015).

[26] A. Sterdyniak, N. R. Cooper, and N. Regnault, Bosonic integer quantum Hall effect in optical flux lattices, Phys. Rev. Lett. **115**, 116802 (2015).

[27] B. Andrews and G. Möller, Stability of fractional Chern insulators in the effective continuum limit of Harper-Hofstadter bands with Chern number $|C| > 1$, Phys. Rev. B **97**, 035159 (2018).

[28] B. Andrews, M. Raja, N. Mishra, M. P. Zaletel, and R. Roy, Stability of fractional Chern insulators with a non-Landau level continuum limit, Phys. Rev. B **109**, 245111 (2024).

[29] Y.-C. He, F. Grusdt, A. Kaufman, M. Greiner, and A. Vishwanath, Realizing and adiabatically preparing bosonic integer and fractional quantum Hall states in optical lattices, Phys. Rev. B **96**, 201103(R) (2017).

[30] P. Rosson, M. Lubasch, M. Kiffner, and D. Jaksch, Bosonic fractional quantum Hall states on a finite cylinder, Phys. Rev. A **99**, 033603 (2019).

[31] F. A. Palm, M. Buser, J. Léonard, M. Aidelsburger, U. Schollwöck, and F. Grusdt, Bosonic Pfaffian state in the Hofstadter-Bose-Hubbard model, Phys. Rev. B **103**, L161101 (2021).

[32] B. Andrews, M. Mohan, and T. Neupert, Abelian topological order of $\nu = 2/5$ and 3/7 fractional quantum Hall states in lattice models, Phys. Rev. B **103**, 075132 (2021).

[33] J. Boesl, R. Dilip, F. Pollmann, and M. Knap, Characterizing fractional topological phases of lattice bosons near the first Mott lobe, Phys. Rev. B **105**, 075135 (2022).

[34] M. Gerster, M. Rizzi, P. Silvi, M. Dalmonte, and S. Montangero, Fractional quantum Hall effect in the interacting Hofstadter model via tensor networks, Phys. Rev. B **96**, 195123 (2017).

[35] E. Macaluso, T. Comparin, R. O. Umucalilar, M. Gerster, S. Montangero, M. Rizzi, and I. Carusotto, Charge and statistics of lattice quasiholes from density measurements: A tree tensor network study, Phys. Rev. Res. **2**, 013145 (2020).

[36] J. Jordan, R. Orús, G. Vidal, F. Verstraete, and J. I. Cirac, Classical simulation of infinite-size quantum lattice systems in two spatial dimensions, Phys. Rev. Lett. **101**, 250602 (2008).

[37] R. J. Baxter, Dimers on a rectangular lattice, J. Math. Phys. **9**, 650 (1968).

[38] R. J. Baxter, Variational approximations for square lattice models in statistical mechanics, J. Stat. Phys. **19**, 461 (1978).

[39] T. Nishino and K. Okunishi, Corner transfer matrix renormalization group method, J. Phys. Soc. Jpn. **65**, 891 (1996).

[40] T. Nishino and K. Okunishi, Corner transfer matrix algorithm for classical renormalization group, J. Phys. Soc. Jpn. **66**, 3040 (1997).

[41] R. Orús and G. Vidal, Simulation of two-dimensional quantum systems on an infinite lattice revisited: Corner transfer matrix for tensor contraction, Phys. Rev. B **80**, 094403 (2009).

[42] P. Corboz, J. Jordan, and G. Vidal, Simulation of fermionic lattice models in two dimensions with projected entangled-pair states: Next-nearest neighbor Hamiltonians, Phys. Rev. B **82**, 245119 (2010).

[43] P. Corboz, S. R. White, G. Vidal, and M. Troyer, Stripes in the two-dimensional $t-J$ model with infinite projected entangled-pair states, Phys. Rev. B **84**, 041108(R) (2011).

[44] P. Corboz, T. M. Rice, and M. Troyer, Competing states in the $t-J$ model: Uniform d-wave state versus stripe state, Phys. Rev. Lett. **113**, 046402 (2014).

[45] H. Li and F. D. M. Haldane, Entanglement spectrum as a generalization of entanglement entropy: Identification of topological order in non-Abelian fractional quantum Hall effect states, Phys. Rev. Lett. **101**, 010504 (2008).

[46] J. Haegeman and F. Verstraete, Diagonalizing transfer matrices and matrix product operators: A medley of exact and computational methods, Annu. Rev. Condens. Matter Phys. **8**, 355 (2017).

[47] See Supplemental Material at http://link.aps.org/supplemental/10.1103/PhysRevB.109.L241117 for more details, which also includes Refs. [60,80–85].

[48] P. Corboz, Variational optimization with infinite projected entangled-pair states, Phys. Rev. B **94**, 035133 (2016).

[49] L. Vanderstraeten, J. Haegeman, P. Corboz, and F. Verstraete, Gradient methods for variational optimization of projected entangled-pair states, Phys. Rev. B **94**, 155123 (2016).

[50] H.-J. Liao, J.-G. Liu, L. Wang, and T. Xiang, Differentiable programming tensor networks, Phys. Rev. X **9**, 031041 (2019).

[51] J. Naumann, E. L. Weerda, M. Rizzi, J. Eisert, and P. Schmoll, An introduction to infinite projected entangled-pair state methods for variational ground state simulations using automatic differentiation, arXiv:2308.12358.

[52] J. Hasik, D. Poilblanc, and F. Becca, Investigation of the Néel phase of the frustrated Heisenberg antiferromagnet by differentiable symmetric tensor networks, SciPost Phys. **10**, 012 (2021).

[53] J. Hasik, G. B. Mbeng, S. Capponi, F. Becca, and A. M. Läuchli, Symmetric projected entangled-pair states analysis of a phase transition in coupled spin-$\frac{1}{2}$ ladders, Phys. Rev. B **106**, 125154 (2022).

[54] S. Niu, J. Hasik, J.-Y. Chen, and D. Poilblanc, Chiral spin liquids on the kagome lattice with projected entangled simplex states, Phys. Rev. B **106**, 245119 (2022).

[55] E. Tang, J.-W. Mei, and X.-G. Wen, High-temperature fractional quantum Hall states, Phys. Rev. Lett. **106**, 236802 (2011).

[56] T. Neupert, L. Santos, C. Chamon, and C. Mudry, Fractional quantum Hall states at zero magnetic field, Phys. Rev. Lett. **106**, 236804 (2011).
[57] K. Sun, Z. Gu, H. Katsura, and S. Das Sarma, Nearly flatbands with nontrivial topology, Phys. Rev. Lett. **106**, 236803 (2011).
[58] M. Aidelsburger, Artificial gauge fields and topology with ultracold atoms in optical lattices, J. Phys. B: At. Mol. Opt. Phys. **51**, 193001 (2018).
[59] J. I. Cirac, D. Poilblanc, N. Schuch, and F. Verstraete, Entanglement spectrum and boundary theories with projected entangled-pair states, Phys. Rev. B **83**, 245134 (2011).
[60] L. Cincio and G. Vidal, Characterizing topological order by studying the ground states on an infinite cylinder, Phys. Rev. Lett. **110**, 067208 (2013).
[61] M. J. Arildsen and A. W. W. Ludwig, Generalized Gibbs ensemble description of real-space entanglement spectra of $(2+1)$-dimensional chiral topological systems with SU(2) symmetry, Phys. Rev. B **106**, 035138 (2022).
[62] J. K. Jain, Composite-fermion approach for the fractional quantum Hall effect, Phys. Rev. Lett. **63**, 199 (1989).
[63] T. Senthil and M. Levin, Integer quantum Hall effect for bosons, Phys. Rev. Lett. **110**, 046801 (2013).
[64] S. Furukawa and M. Ueda, Integer quantum Hall state in two-component Bose gases in a synthetic magnetic field, Phys. Rev. Lett. **111**, 090401 (2013).
[65] G. Möller and N. R. Cooper, Fractional Chern insulators in Harper-Hofstadter bands with higher Chern number, Phys. Rev. Lett. **115**, 126401 (2015).
[66] L. A. Ponomarenko, R. V. Gorbachev, G. L. Yu, D. C. Elias, R. Jalil, A. A. Patel, A. Mishchenko, A. S. Mayorov, C. R. Woods, J. R. Wallbank *et al.*, Cloning of Dirac fermions in graphene superlattices, Nature (London) **497**, 594 (2013).
[67] E. J. Bergholtz and Z. Liu, Topological flat band models and fractional Chern insulators, Int. J. Mod. Phys. B **27**, 1330017 (2013).
[68] Y.-H. Zhang, D. N. Sheng, and A. Vishwanath, SU(4) chiral spin liquid, exciton supersolid, and electric detection in moiré bilayers, Phys. Rev. Lett. **127**, 247701 (2021).
[69] Y.-M. Wu, Z. Wu, and H. Yao, Pair-density-wave and chiral superconductivity in twisted bilayer transition metal dichalcogenides, Phys. Rev. Lett. **130**, 126001 (2023).
[70] F. Wu, T. Lovorn, E. Tutuc, and A. H. MacDonald, Hubbard model physics in transition metal dichalcogenide moiré bands, Phys. Rev. Lett. **121**, 026402 (2018).
[71] L. Wang, E.-M. Shih, A. Ghiotto, L. Xian, D. A. Rhodes, C. Tan, M. Claassen, D. M. Kennes, Y. Bai, B. Kim, K. Watanabe, T. Taniguchi, X. Zhu, J. Hone, A. Rubio, A. N. Pasupathy, and C. R. Dean, Correlated electronic phases in twisted bilayer transition metal dichalcogenides, Nat. Mater. **19**, 861 (2020).
[72] D. Kiese, Y. He, C. Hickey, A. Rubio, and D. M. Kennes, TMDs as a platform for spin liquid physics: A strong coupling study of twisted bilayer WSe_2, APL Mater. **10**, 031113 (2022).
[73] B. Ponsioen, F. F. Assaad, and P. Corboz, Automatic differentiation applied to excitations with projected entangled pair states, SciPost Phys. **12**, 006 (2022).
[74] B. Ponsioen, J. Hasik, and P. Corboz, Improved summations of n-point correlation functions of projected entangled-pair states, arXiv:2306.13327.
[75] W.-L. Tu, L. Vanderstraeten, N. Schuch, H.-Y. Lee, N. Kawashima, and J.-Y. Chen, Generating function for projected entangled-pair states, PRX Quantum **5**, 010335 (2024).
[76] R. Chi, Y. Liu, Y. Wan, H.-J. Liao, and T. Xiang, Spin excitation spectra of anisotropic spin-$1/2$ triangular lattice Heisenberg antiferromagnets, Phys. Rev. Lett. **129**, 227201 (2022).
[77] E. Weerda and M. Rizzi, Data accompanying Fractional quantum Hall states with variational projected entangled-pair states: A study of the bosonic Harper-Hofstadter model, 10.5281/zenodo.10210305 (2023).
[78] www.gauss-centre.eu.
[79] J. S. Centre, JURECA: Data centric and booster modules implementing the modular supercomputing architecture at Jülich supercomputing centre, J. Res. Facil. **7**, A182 (2021).
[80] M. Hladnik and M. Omladič, Spectrum of the product of operators, Proc. Am. Math. Soc. **102**, 300 (1988).
[81] V. Zauner-Stauber, L. Vanderstraeten, M. T. Fishman, F. Verstraete, and J. Haegeman, Variational optimization algorithms for uniform matrix product states, Phys. Rev. B **97**, 045145 (2018).
[82] J. Haegeman, S. Michalakis, B. Nachtergaele, T. J. Osborne, N. Schuch, and F. Verstraete, Elementary excitations in gapped quantum spin systems, Phys. Rev. Lett. **111**, 080401 (2013).
[83] L. Vanderstraeten, J. Haegeman, and F. Verstraete, Tangent-space methods for uniform matrix product states, SciPost Phys. Lect. Notes, 7 (2019).
[84] M. Van Damme, R. Vanhove, J. Haegeman, F. Verstraete, and L. Vanderstraeten, Efficient matrix product state methods for extracting spectral information on rings and cylinders, Phys. Rev. B **104**, 115142 (2021).
[85] W. X. Gang, *Quantum Field Theory of Many-Body Systems: From the Origin of Sound to an Origin of Light and Electrons* (Oxford University Press, Oxford, 2007).